ican Geophysical Union, Washington, DC, 1998), pp. 153–176.
8. W. Bach, N. R. Banerjee, H. J. B. Dick, E. T. Baker, *Geochem. Geophys. Geosyst.* **3**, GC000279 (2001).
9. H. N. Edmonds *et al.*, *Nature* **421**, 252 (2003).
10. H. J. B. Dick, J. Lin, H. Schouten, *Nature* **426**, 405 (2003).
11. G. L. Früh-Green *et al.*, *Science* **302**, 495 (2003).
12. R. P. Lowell, P. A. Rona, *Geophys. Res. Lett.* **29**, 10.1029/2001GL01411 (2002).
13. T. L. Grove, S. W. Parman, *Earth Planet. Sci. Lett.* **219**, 173 (2004).
14. Materials and methods are available as supporting material on *Science* Online.
15. D. K. Blackman *et al.*, *Marine Geophsy. Res.* **23**, 443 (2004).
16. T. Schroeder, B. John, B. R. Frost, *Geology* **30**, 367 (2002).
17. J. A. Karson, in *Faulting and Magmatism at Mid-Ocean Ridges*, W. R. Buck, P. T. Delaney, J. A. Karson, Y. Lagabrielle, Eds. (Geophysical Monograph 106, American Geophysical Union, Washington, DC, 1998), pp. 177–218.
18. D. S. Kelley, J. A. Baross, J. R. Delaney, *Annu. Rev. Earth Planet. Sci.* **30**, 385 (2002).
19. J. L. Charlou, J. P. Donval, Y. Fouquet, P. Jean-Baptiste, N. Holm, *Chem. Geol.* **191**, 345 (2002).
20. D. R. Janecky, W. E. Seyfried Jr., *Geochim. Cosmochim. Acta* **50**, 1357 (1986).
21. C. Neal, G. Stanger, *Earth Planet. Sci. Lett.* **66**, 315 (1983).
22. M. E. Berndt, D. Allen, W. E. Seyfried Jr., *Geology* **24**, 351 (1996).
23. L. R. Wetzel, E. L. Shock, *J. Geophys. Res.* **105**, 8319 (2000).
24. T. M. McCollom, J. S. Seewald, *Geochim. Cosmochim. Acta* **65**, 3769 (2001).
25. M. D. Lilley *et al.*, *Nature* **364**, 45 (1993).
26. J. A. Welhan, H. Craig, *Eos* **60**, 863 (1979).
27. J. A. Welhan, H. Craig, in *Hydrothermal Processes at Seafloor Spreading Centers*, A. Rona Peter, K. Bostrom, L. Laubier, L. Smith Kenneth Jr., Eds. (Plenum, New York, 1983), pp. 391–409.
28. P. Fritz, I. D. Clark, J. C. Fontes, M. J. Whiticar, E. Faber, in *Proceedings of the 7th International Symposium on Water-Rock Interaction; Volume 1, Low Temperature Environments*, K. Kharaka Yousif, S. Maest Ann, Eds. (International Association of Geochemistry and Cosmochemistry and Alberta Research Council, Sub-Group on Water-Rock Interaction, Edmonton, Alberta, Canada, 1992), pp. 793–796.
29. T. A. Abrajano *et al.*, *Chem. Geol.* **71**, 211 (1988).
30. M. O. Schrenk, D. S. Kelley, S. A. Bolton, J. A. Baross, *Environ. Microbiol.* **6**, 1086 (2004).
31. A.-L. Reysenbach, D. Götz, D. Yernool, in *Biodiversity of Microbial Life*, J. T. Staley, A.-L. Reysenbach, Eds. (Wiley-Liss, New York, 2002), pp. 345–422.
32. J. M. Hayes, J. W. Valley, D. R. Cole, Eds., *Stable Isotope Geochemistry, Reviews in Mineralogy and Geochemistry* (Mineralogical Society of America, Washington, DC, 2001), vol. 43, chap. 3.
33. K. U. Hinrichs, R. E. Summons, V. Orphan, S. P. Sylva, J. M. Hayes, *Org. Geochem.* **31**, 1685 (2000).
34. V. Orphan *et al.*, *Proc. Natl. Acad. Sci. U.S.A.* **99**, 7663 (2002).
35. V. Tunnicliffe, C. M. R. Fowler, *Nature* **379**, 531 (1996).
36. A. V. Gebruk, S. V. Galkin, A. L. Vereshchaka, L. I. Moskalev, A. J. Southward, *Adv. Mar. Biol.* **32**, 93 (1997).
37. A. A. Suror, E. H. Arfa, *J. Afr. Earth Sci.* **24**, 315 (1997).
38. B. E. Treves, G. D. Harper, *Ofioliti* **19b**, 435 (1994).
39. M. M. Mottl, S. C. Komor, P. Fryer, C. L. Moyer, *Geochem. Geophys. Geosyst.* **4**, 11 (2003).
40. P. Fryer, C. G. Wheat, M. J. Mottl, *Geology* **27**, 103 (1997).
41. E. Gracia, J. L. Charlou, J. Radford-Knoery, L. Parson, *Earth Planet. Sci. Lett.* **177**, 89 (2000).
42. J. L. Charlou, J. P. Donval, Y. Fouquet, P. Jean-Baptiste, N. Holm, *Chem. Geol.* **191**, 345 (2002).
43. E. Bonatti, P. J. Michael, *Earth Planet. Sci. Lett.* **91**, 297 (1989).
44. T. J. Reston *et al.*, *Geology* **29**, 587 (2001).
45. E. L. Shock, M. D. Schulte, *J. Geophys. Res.* **103**, 28,513 (1998).
46. H. A. Schmidt, K. Strimmer, M. Vingron, A. von Haeseler, *Bioinformatics* **18**, 502 (2002).

47. We express our deep appreciation to the crews of the R/V *Atlantis* and *Alvin* for their support and help with the 2003 Lost City expedition. Their humor, friendship, and professionalism were instrumental to the success of the field program. We also very much appreciate the helpful comments of four anonymous reviewers. We thank B. Nelson for his time and help with the Sr analyses and for making his laboratory available to us, S. R. Emerson for guidance in chemical analyses of the carbonate samples and use of his laboratory facilities, and M. Lin for technical assistance with phylogenetic analyses. We acknowledge funding from NSF grants OCE0137206 (D.S.K.), OCE0136816 (J.A.K.), and OCE0136871 (D.R.Y. and T.M.S.). Work by J.A.B. was also supported by the NASA Astrobiology Institute through the Carnegie Geophysical Institute. Support to G.L.F.-G. was through Swiss National Science Foundation grant 2100-068055. J.M.H. was supported in part by the NASA Astrobiology Institute through the University of Rhode Island.

Supporting Online Material
www.sciencemag.org/cgi/content/full/307/5714/1428/DC1
Materials and Methods
SOM Text
Figs. S1 and S2
Table S1
References
Movies S1 and S2

9 July 2004; accepted 21 January 2005
10.1126/science.1102556

The Influence of *CCL3L1* Gene–Containing Segmental Duplications on HIV-1/AIDS Susceptibility

Enrique Gonzalez,[1]* Hemant Kulkarni,[1]* Hector Bolivar,[1]*† Andrea Mangano,[2]* Racquel Sanchez,[1]‡ Gabriel Catano,[1]‡ Robert J. Nibbs,[3]‡ Barry I. Freedman,[4]‡ Marlon P. Quinones,[1]‡ Michael J. Bamshad,[5] Krishna K. Murthy,[6] Brad H. Rovin,[7] William Bradley,[8,9] Robert A. Clark,[1] Stephanie A. Anderson,[8,9] Robert J. O'Connell,[9,10] Brian K. Agan,[9,10] Seema S. Ahuja,[1] Rosa Bologna,[11] Luisa Sen,[2] Matthew J. Dolan,[9,10,12]§ Sunil K. Ahuja[1]§

Segmental duplications in the human genome are selectively enriched for genes involved in immunity, although the phenotypic consequences for host defense are unknown. We show that there are significant interindividual and interpopulation differences in the copy number of a segmental duplication encompassing the gene encoding CCL3L1 (MIP-1αP), a potent human immunodeficiency virus–1 (HIV-1)–suppressive chemokine and ligand for the HIV coreceptor CCR5. Possession of a *CCL3L1* copy number lower than the population average is associated with markedly enhanced HIV/acquired immunodeficiency syndrome (AIDS) susceptibility. This susceptibility is even greater in individuals who also possess disease-accelerating *CCR5* genotypes. This relationship between *CCL3L1* dose and altered HIV/AIDS susceptibility points to a central role for CCL3L1 in HIV/AIDS pathogenesis and indicates that differences in the dose of immune response genes may constitute a genetic basis for variable responses to infectious diseases.

Duplicated host defense genes that are known to have dosage effects are thought to contribute to the genetic basis of some complex diseases, although direct evidence for this is lacking. We surmised that a hotspot for segmental duplications on human chromosome 17q might be relevant to immunity against infectious diseases such as HIV-1 because it encompasses two CC chemokine genes, CC chemokine ligand 3-like 1 (*CCL3L1*; other names, *MIP-1αP* and *LD78*β) and *CCL4L1* (*MIP-1*β*-like*), which represent the duplicated isoforms of the genes encoding CCL3 and CCL4, respectively (*1*–*3*). As a consequence of these duplications, the copy number of *CCL3L1* and *CCL4L1* varies among individuals (*2*, *3*) (fig. S1A). This is important because CCL3L1 is the most potent known ligand for CC chemokine receptor 5 (CCR5), the major coreceptor for HIV, and it is a dominant HIV-suppressive chemokine (*3*).

In light of this relationship between CCL3L1 and its in vitro effect on HIV infection, we selected HIV infection as a model system in which to test our hypothesis that segmental duplications causing dosage effects of host defense genes are associated with phenotypic effects in vivo. To test this hypothesis, we determined the distribution of chemokine gene–containing segmental duplications in 1064 humans from 57 populations and 83 chimpanzees (*4*). We next analyzed 4308 HIV-1–positive (HIV^+) and HIV-1–negative (HIV^-) individuals from groups with different geographical ancestries (e.g., Africans and Europeans) to determine if the risk of acquiring HIV and the rate at which HIV disease progressed were sensitive to differences in the dose of *CCL3L1*

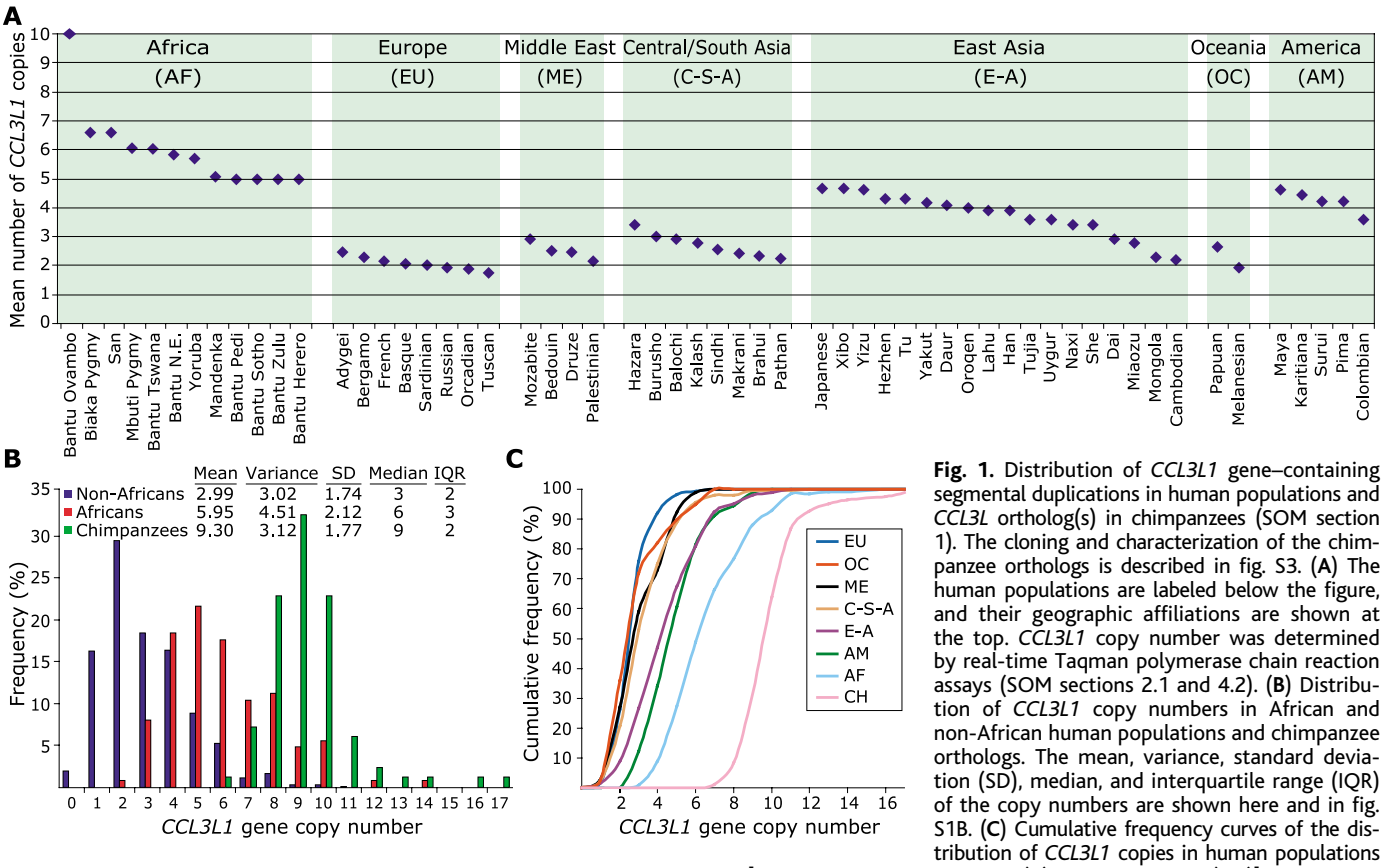

Fig. 1. Distribution of *CCL3L1* gene–containing segmental duplications in human populations and *CCL3L* ortholog(s) in chimpanzees (SOM section 1). The cloning and characterization of the chimpanzee orthologs is described in fig. S3. (**A**) The human populations are labeled below the figure, and their geographic affiliations are shown at the top. *CCL3L1* copy number was determined by real-time Taqman polymerase chain reaction assays (SOM sections 2.1 and 4.2). (**B**) Distribution of *CCL3L1* copy numbers in African and non-African human populations and chimpanzee orthologs. The mean, variance, standard deviation (SD), median, and interquartile range (IQR) of the copy numbers are shown here and in fig. S1B. (**C**) Cumulative frequency curves of the distribution of *CCL3L1* copies in human populations from different geographic regions and chimpanzee. The order of the abbreviations [geographic regions shown in (A) and chimpanzee (CH)] matches the order of the cumulative frequency curves from left to right.

gene–containing segmental duplications (*4*) [supporting online material (SOM) section 4.1].

Nonrandom distribution of *CCL3L1*-containing segmental duplications. African populations possessed a significantly greater number of *CCL3L1* gene copies than non-Africans (Fig. 1 and fig. S1B). The geographic region of origin explained nearly 35% of the total variation in the distribution of *CCL3L1* gene copies (analysis of variance: $F = 94.41$, df = 6, 1037; $P = 1.23 \times 10^{-94}$). Corroborating this, in separate cohorts of HIV$^-$ subjects, there were significant interindividual and interpopulation differences in *CCL3L1* copy numbers. The median copy number in HIV$^-$ Argentinean children was two, and in HIV$^-$ African-American (AA), European-American (EA), and Hispanic-American (HA) adults, it was four, two, and three, respectively (Fig. 2, A to D, open bars, and fig. S2).

The duplicated region encoding human CCL3L1 had an ancestral correlate in chimpanzee (Fig. 1 and fig. S3). Together, these results demonstrated that there were significant differences between species and among human populations in the frequency of chemokine gene–containing segmental duplications (Fig. 1, B and C). Despite these differences, the dispersion around the average copy number was similar in both human populations and chimpanzees (Fig. 1B and fig. S1B). On the basis of these observations, we hypothesized that it is not the absolute copy number per se, but rather the gene dose relative to the average copy number in each population that confers HIV/AIDS susceptibility.

***CCL3L1* gene dose and HIV/AIDS susceptibility.** Several lines of evidence, from four different human populations and in the setting of two different modes of acquiring HIV (i.e., mother-to-child and adult-to-adult), indicated that possession of a low *CCL3L1* copy number was a major determinant of enhanced HIV susceptibility among individuals. Individuals with a low *CCL3L1* copy number were overrepresented among the HIV$^+$ compared with HIV$^-$ subjects (shift to the left in Fig. 2, A to D, and figs. S2 and S4). On the basis of the consistency, strength, and significance of the differences in the distribution of *CCL3L1* copy numbers in the HIV$^+$ and HIV$^-$ individuals in each of the cohorts studied, we rejected the null hypothesis of no association between risk of acquiring HIV and *CCL3L1* copy number (Fig. 2, A to D, and fig. S2).

We next determined the strength of the association between *CCL3L1* copy number and risk of acquiring HIV (Fig. 2, E to H). In our initial analyses, we chose the population-specific median copy number in the uninfected group as a reference point to compute the risk of acquiring HIV (SOM section 5.1). Compared with possession of two copies of *CCL3L1*, children possessing less than two or more than two copies had significantly higher or lower risks, respectively, of acquiring HIV (Fig. 2E). This association was

[1]Veterans Administration Research Center for AIDS and HIV-1 Infection, South Texas Veterans Health Care System, and Department of Medicine, University of Texas Health Science Center, San Antonio, TX 78229, USA. [2]Laboratorio de Biología Celular y Retrovirus–Consejo Nacional de Investigaciones Científicus y Tecnicas, and [11]Servicio de Infectología, Hospital de Pediatría "J. P. Garrahan," 1245 Buenos Aires, Argentina. [3]Cancer Research UK Beatson Laboratories, Glasgow G61 1BD, Scotland, UK. [4]Department of Internal Medicine, Wake Forest University School of Medicine, Winston-Salem, NC 27157, USA. [5]Departments of Human Genetics and Pediatrics, University of Utah, Salt Lake City, UT 84112, USA. [6]Southwest Foundation for Biomedical Research, San Antonio, TX 78227, USA. [7]Division of Nephrology, Ohio State University, Columbus, OH 43210, USA. [8]Henry M. Jackson Foundation, [9]Tri-Service AIDS Clinical Consortium, and [10]Infectious Diseases Service, Wilford Hall Medical Center, Lackland Air Force Base, TX 78236, USA. [12]Defense Institute for Medical Operations, Brooks City-Base, TX 78235, USA.

*These authors contributed equally to this work.
†Present address: AIDS Clinical Research Unit, University of Miami, Miller School of Medicine, Miami, FL 33136, USA.
‡These authors contributed equally to this work.
§To whom correspondence should be addressed. E-mail: ahujas@uthscsa.edu (S.K.A.); matthew.dolan@brooks.af.mil (M.J.D.)

evident in the analysis of the entire cohort of children with (table S1A) or without (Fig. 2E) adjustments for receipt of zidovudine prophylaxis given to reduce the risk of transmission and for individuals who received no prophylaxis (table S1A). Notably, with each increase in *CCL3L1* copy number above the median, there was a dose-dependent, stepwise decrease in the risk for acquiring HIV (Fig. 2E). The findings depicted in Fig. 2, F to H, and those derived from a separate analysis in another cohort of 1133 HIV$^-$ individuals matched for ethnicity/race (fig. S2), indicated that adults who possessed a *CCL3L1* copy number lower than the population-specific median were at a higher risk of acquiring HIV. Thus, in each population, the median number of *CCL3L1* copies served as the transition point at which the balance tilted in favor of protection against acquiring HIV.

We also estimated the risk of acquiring HIV across the cline of population-specific high to low *CCL3L1* copy numbers (fig. S4). Depending on the study population, each *CCL3L1* copy lowered the risk of acquiring HIV by 4.5 to 10.5%, indicating that the population-specific high and low *CCL3L1* copy numbers are at different ends of a distribution of HIV susceptibility (SOM section 5.2). Substantiating this, relative to possession of the population-specific high *CCL3L1* copy numbers shown in fig. S4, individuals who had a low copy number had between 69 and 97% higher risk of acquiring HIV (fig. S4).

The aforementioned analyses were conducted with logistic regression. Although membership in either the HIV$^+$ or HIV$^-$ group is not a random outcome, to the extent that these two groups can be thought of as random samples from their respective subsets of a well-defined population, logistic regression on group membership allows estimation of the relative odds of being HIV$^+$ or HIV$^-$ for two different copy numbers. In this sense, logistic regression permits the determination of the association between *CCL3L1* copy number and risk of acquiring HIV. Because the number of *CCL3L1* copies followed a Poisson distribution, we also used Poisson regression analysis to determine the association between *CCL3L1* copy number and risk of acquiring HIV infection. These analyses assume that copy numbers are conditional on HIV status and show that HIV$^+$ subjects have significantly lower *CCL3L1* copy numbers than do HIV$^-$ subjects (Fig. 2I). Although the true risk of HIV acquisition associated with possession of different *CCL3L1* gene copy numbers can theoretically only be estimated from a longitudinal study, in the cohorts we studied, the results of two different statistical approaches demonstrate a strong association between possession of low *CCL3L1* copy number and risk of acquiring HIV infection (Fig. 2, E and J, and table S1B).

In addition to influencing HIV acquisition, the number of *CCL3L1* copies was associated with variable rates of disease progression (figs. S5 and S6). For example, in the adult HIV$^+$ cohort, a gene dose lower than the overall cohort median or population-specific median was associated with a dose-dependent increased risk of progressing rapidly to AIDS or death (Fig. 3, A and B, and figs. S5). A disease-influencing effect of *CCL3L1* dose was not detected in the HIV$^+$ children, suggesting either that the roles of CCL3L1 in HIV$^+$ adults and children differ or that the

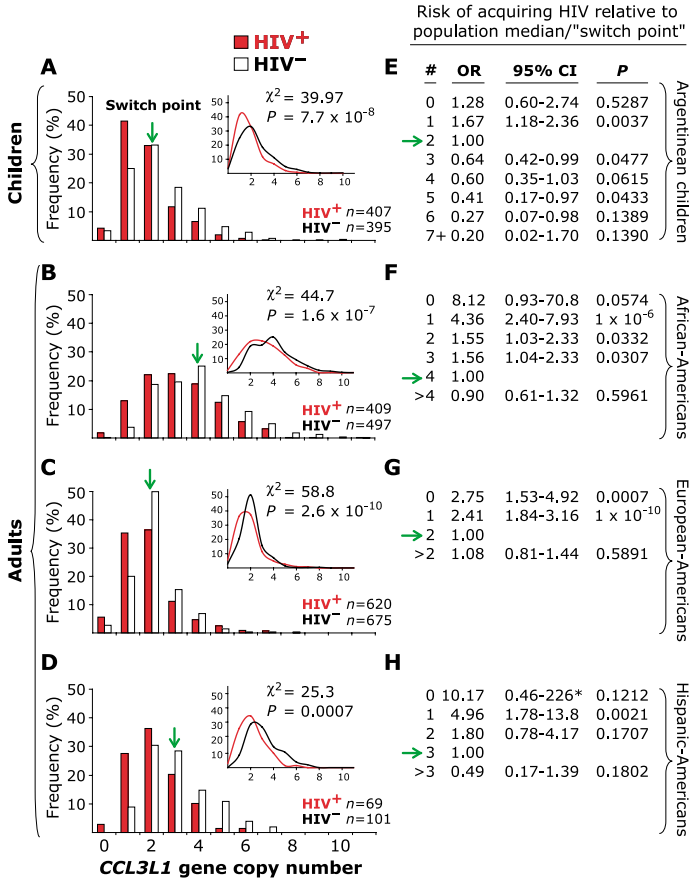

Risk of acquiring HIV relative to population median/"switch point"

	#	OR	95% CI	P	
E	0	1.28	0.60-2.74	0.5287	Argentinean children
	1	1.67	1.18-2.36	0.0037	
	→2	1.00			
	3	0.64	0.42-0.99	0.0477	
	4	0.60	0.35-1.03	0.0615	
	5	0.41	0.17-0.97	0.0433	
	6	0.27	0.07-0.98	0.1389	
	7+	0.20	0.02-1.70	0.1390	
F	0	8.12	0.93-70.8	0.0574	African-Americans
	1	4.36	2.40-7.93	1 x 10⁻⁶	
	2	1.55	1.03-2.33	0.0332	
	3	1.56	1.04-2.33	0.0307	
	→4	1.00			
	>4	0.90	0.61-1.32	0.5961	
G	0	2.75	1.53-4.92	0.0007	European-Americans
	1	2.41	1.84-3.16	1 x 10⁻¹⁰	
	→2	1.00			
	>2	1.08	0.81-1.44	0.5891	
H	0	10.17	0.46-226*	0.1212	Hispanic-Americans
	1	4.96	1.78-13.8	0.0021	
	2	1.80	0.78-4.17	0.1707	
	→3	1.00			
	>3	0.49	0.17-1.39	0.1802	

I

#	HIV$^+$ subjects		HIV$^-$ subjects	
	Subjects	*CCL3L1* gene copies Mean (95% CI)	Subjects	*CCL3L1* gene copies Mean (95% CI)
1.	Arg. children	1.85 (1.72–1.99)	Arg. children	2.41 (2.26–2.57)
2.	WHMC EA+HA	1.88 (1.74–1.99)	WHMC EA+HA	2.10 (1.99–2.22)
3.	WHMC AA	3.26 (3.08–3.44)	WHMC AA	3.79 (3.60–3.98)
4.	WHMC EA	1.86 (1.75–1.97)	Non-WHMC EA	2.13 (2.02–2.24)
5.	WHMC AA	3.26 (3.08–3.44)	Non-WHMC AA	3.90 (3.73–4.08)
6.	WHMC HA	2.06 (1.73–2.43)	Non-WHMC HA	3.08 (2.75–3.44)

J

#	Poisson regression			Logistic regression		
	RR	95% CI	P	OR	95% CI	P
1.	0.77	0.70-0.85	6.7 x 10⁻⁷	0.71	0.63–0.80	6.7 x 10⁻⁹
2.	0.90	0.83-0.97	0.0059	0.83	0.75–0.92	0.0005
3.	0.86	0.80-0.93	6.6 x 10⁻⁵	0.81	0.74–0.88	3.3 x 10⁻⁶
4.	0.87	0.81-0.95	0.0007	0.80	0.72–0.89	2.2 x 10⁻⁵
5.	0.84	0.78-0.90	4.7 x 10⁻⁷	0.78	0.72–0.85	8.4 x 10⁻⁹
6.	0.67	0.55-0.82	8.5 x 10⁻⁵	0.49	0.36–0.67	9.0 x 10⁻⁶

Fig. 2. *CCL3L1* dose and risk of acquiring HIV-1. (**A** to **D**) Histograms and the cubic-spline smoothed frequency curves (insets) show that the distribution of the *CCL3L1* copy numbers (*x* axis) in HIV$^+$ (red bars or red lines in inset) versus HIV$^-$ (open bars or black line in inset) individuals is markedly different (χ^2 and *P* values above insets; *n* = number of individuals in each group). Vertical green arrow indicates the switch point (copy number at which the HIV$^+$/HIV$^-$ ratio switched from >1 to ≤1) (SOM section 5.1). The cohort of Argentinean children is composed of children exposed perinatally to HIV (*4*). The HIV$^+$ adults from the indicated ethnic/racial groups (noted on the right) are from the Wilford Hall Medical Center (WHMC) cohort (*14*) and are compared with a control group from the general population that is matched for ethnicity/race (*4*). (**E** to **H**) Risk of acquiring HIV relative to the population-specific median [horizontal arrow; odds ratio (OR) = 1] was determined by multivariate logistic regression analyses. *, Jewell correction (*4*); #, *CCL3L1* gene copy number; CI, confidence interval; *P*, significance value. (**I**) Distribution of *CCL3L1* copies in the indicated subject groups (Poisson means and exact 95% CI). #, group number. Arg., Argentinean. SOM section 1.1 provides details of these study groups. In the HIV$^-$ WHMC cohort, as HAs were categorized with EAs, they were placed within a single group (WHMC EA + HA) and compared with subjects from the HIV$^+$ WHMC cohort that are matched for ethnicity/race. (**J**) Results of Poisson and logistic regression models in the study groups indicated in (I) (#1 to 6) for the association between *CCL3L1* copies and risk of acquiring HIV infection were comparable (table S1B). RR, relative risk.

short follow-up time in the pediatric cohort was insufficient to detect an effect.

Mechanistic links between *CCL3L1* dose and HIV/AIDS susceptibility. Increasing *CCL3L1* copy number was positively associated with CCL3/CCL3L1 secretion and negatively associated with the proportion of CD4$^+$ T cells that express CCR5 (Fig. 3, C and D) (*2*). Additionally, there was a dose-dependent association between *CCL3L1* copy number and the viral set point and rate of change in CD4$^+$ T cell counts, two well-established predictors of clinical outcome (*5*); low *CCL3L1* doses were associated with a higher viral set point and greater subsequent T cell loss (Fig. 3, E and F). These relationships might explain the association between *CCL3L1* gene dose and risk of acquiring HIV and disease progression given that (i) chemokines are thought to mediate their HIV-suppressive activity by steric blocking of the interaction between glycoprotein (gp) 120 and CCR5 or ligand-mediated internalization of CCR5, reducing its availability for use by gp 120 (*3*), and (ii) high CCR5 ligand and/or low CCR5 receptor expression represents a correlate of HIV/AIDS protection (*6*–*12*).

Phenotypic equivalency of population-specific *CCL3L1* gene doses. Human populations differ in their *CCL3L1* gene content (Fig. 1). Accordingly, it was important to determine whether an absolute *CCL3L1* copy number (e.g., two copies) was associated with similar transmission- and/or disease-influencing phenotypic effects in different populations. To do so, we compared the associated phenotypic effects of similar and dissimilar *CCL3L1* copy numbers in HIV$^+$ EAs and AAs (Fig. 3, G to N), and the change in the frequency distribution of copy number in these two populations over time (Fig. 3, O and P). The findings indicated that in HIV$^+$ EAs and AAs, the *CCL3L1* copy numbers that corresponded to the population-specific median, half-median, and low doses (i) were associated with comparable rates of disease progression or changes in CD3$^+$, CD4$^+$, or CD8$^+$ T cell counts (Fig. 3, G to N, and table S2), and (ii) had similar trajectories with respect to the changes in their distribution profiles over time (Fig. 3, O and P, and figs. S7 and S8). By contrast, possession of two *CCL3L1* copies (i.e., the median and half-median gene dose in EAs and AAs, respectively) was associated with differing rates of disease progression (Fig. 3K). Consistent with this finding, the trajectories of the change in the frequency distribution of individuals possessing two *CCL3L1* copies differed over time: increasing in HIV$^+$ EAs, but declining in HIV$^+$ AAs (Fig. 3, O and P). These findings, together with those shown in Fig. 2 and SOM section 5.1, collectively support the concept that different *CCL3L1* gene doses among populations are associated with phenotypically similar effects (Fig. 3Q).

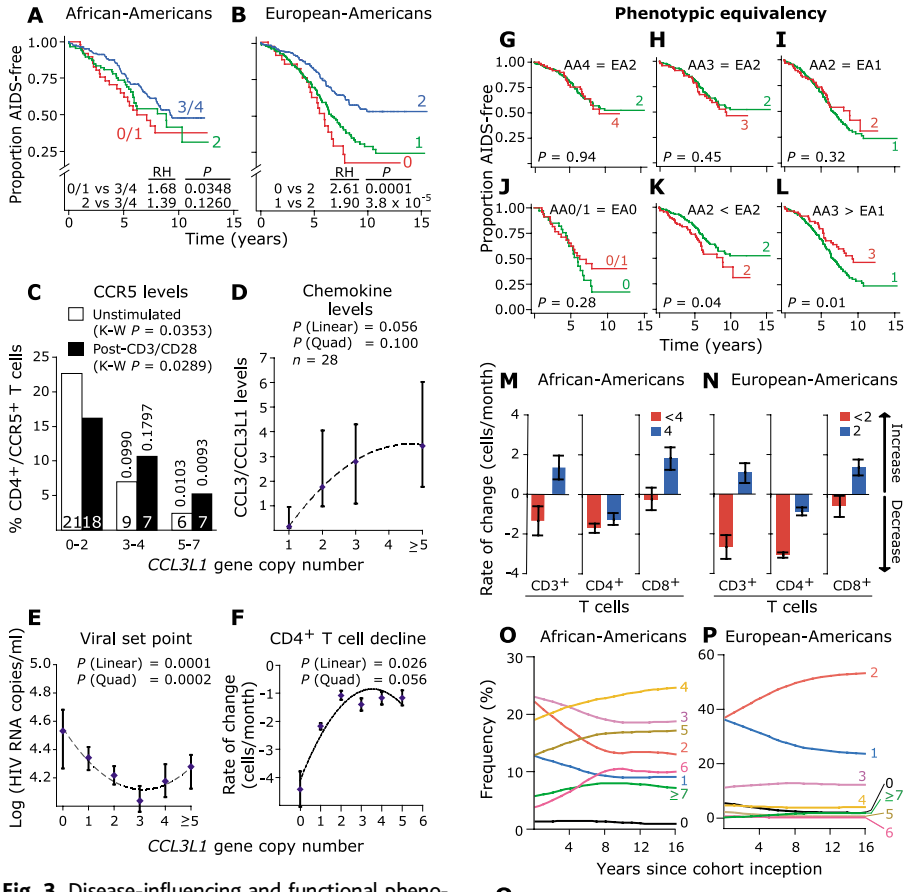

Fig. 3. Disease-influencing and functional phenotypic effects associated with number of *CCL3L1* copies. (**A** and **B**) Kaplan-Meier (KM) survival curves of the development of AIDS in (A) AAs and (B) EAs from the adult WHMC HIV$^+$ cohort who possess a *CCL3L1* copy number equal to or lower than the population-specific median (copy numbers noted adjacent to KM curves). As the population-specific median number of *CCL3L1* copies was three and four in HIV$^+$ and HIV$^-$ AAs, respectively, these two copy numbers were used as the reference genetic strata in (A); the reference group in EAs is two copies. *P* and relative hazard (RH) below the KM curves were determined by Cox proportional hazard models. Overall log-rank significance values and 95% CI for the RHs are shown in fig. S5. (**C**) Relationship between number of *CCL3L1* copies and percentage of CD4$^+$/CCR5$^+$ cells in unstimulated (open bars) or anti-CD3/CD28–stimulated peripheral blood mononuclear cells (black bars). Numbers inside the bars denote the number of individual blood samples studied with the indicated copy numbers. K-W *P*, overall Kruskal-Wallis test *P* value. Vertically oriented numbers indicate *P* values by the Mann-Whitney test for comparison of possession of zero to two versus three to four or five to seven *CCL3L1* copies within each experimental condition. (**D** to **F**) Second-order polynomial regression curves show that (D) CCL3/CCL3L1 concentrations in supernatants of freshly isolated peripheral blood mononuclear cells [for units, see (*4*); *n* = number of individuals], (E) baseline log viral RNA (viral set point), and (F) monthly CD4$^+$ T cell loss have a threshold-type association with *CCL3L1* copies (SOM sections 4.5 to 4.7). (D) and (E) depict medians (±1.7 SD of medians), and (F) depicts 95% CI around the point estimates of the regression coefficients obtained by the General Estimating Equations (GEE) method (*4*). *P* linear and quadratic (quad) indicate significance values for the linear and quadratic terms in the polynomial regression equation, respectively. (**G** to **L**) KM curves of the development of AIDS in HIV$^+$ AAs (red) and EAs (green) who possess a similar or dissimilar *CCL3L1* copy number. The disease-influencing effects associated with possession of [(G) and (H)] median, (I) half-median, and (J) low/null *CCL3L1* doses were similar in EAs and AAs. However, the disease-influencing effects of possession of (K) two copies in AAs (half-median dose in HIV$^-$ AAs) and EAs (median dose) or (L) three copies in AAs (median in HIV$^+$ AAs) and one copy in EAs (half-median in EAs) were not equivalent [see (A) regarding differences in median copy numbers in HIV$^-$ and HIV$^+$ AAs]. Numbers adjacent to the population designators AA and EA indicate the number of copies (e.g., AA4 indicates four copies in AAs). *P* values indicate significance value by log-rank test. =, >, or < indicates the direction of the associated effects. (**M** and **N**) Direction and magnitude of the rate of change in CD3$^+$, CD4$^+$, and CD8$^+$ T cell counts are similar in HIV$^+$ EAs and AAs who possess a *CCL3L1* copy number equal to or lower than the population-specific median (error bars indicate 95% CI; table S2). (**O** and **P**) Results of discrete-time Markov modeling of the evolution of changes in the frequency distribution of *CCL3L1* copy numbers in infinite-sized AA and EA cohorts over 15 years (SOM section 4.8). Numbers adjacent to the curves indicate *CCL3L1* copy numbers. (**Q**) Schema of phenotypic equivalency of the risk of acquiring HIV and disease-influencing effects of population-specific *CCL3L1* doses in EAs and AAs.

They also imply that the phenotypic effects associated with *CCL3L1* gene dosage cannot be estimated by knowing only the absolute *CCL3L1* copy number. This value, in any given individual, is meaningful only if compared with the distribution of *CCL3L1* copies in the geographic ancestral population of the given individual (SOM section 5.1).

Distribution of *CCL3L1* gene copies under HIV selective pressure. The association between *CCL3L1* gene dose and HIV/AIDS susceptibility in adults (Figs. 2 and 3, A and B) predicts that the following pattern should be discernable in a prospective longitudinal cohort in which subjects are recruited at an early stage of infection. Initially, the HIV$^+$ cohort will be enriched for individuals with *CCL3L1* copy numbers lower than the population-specific median. Over time, the prevalence of these individuals will decrease because of their rapid progression to AIDS/death. As a result, the prevalence of HIV$^+$ subjects with *CCL3L1* copy numbers equal to or greater than the population-specific median will increase. Thus, with increasing follow-up times, the distribution of *CCL3L1* copies will begin to resemble that found in HIV$^-$ subjects. The value of testing this prediction is that it combines into a single analytical model the analyses of (i) the susceptibility to infection in individuals with different numbers of *CCL3L1* copies, and (ii) the time to equilibrium between the virus and *CCL3L1* genotype–dependent events in the infected host. Our results are consistent with these predictions (Fig. 3, O and P, and figs. S7 to S9). These observations suggest that infection with HIV-1 can exert a negative selective pressure on individuals with low copy numbers that, depending on the strength of this effect in the general population, could change the population-specific distribution of *CCL3L1* copy number.

***CCL3L1* dose and *CCR5* genotypes in HIV/AIDS susceptibility.** We and others have shown that *CCR5* haplotypes that include *CCR5* promoter polymorphisms as well as coding polymorphisms in *CCR2* (CCR2-V64I) and *CCR5* (Δ*32*) influence the risk of acquiring HIV and the rate of disease progression (*12*–*15*). However, CCR5 is part of a complex system in which virus interacts with CCR5 and CCR5 interacts with various ligands. Thus, if gene-gene interactions are not considered, these interactions might complicate analysis of the in vivo contributions of *CCR5* genotypes. This concern is made all the more apparent by the observation that CCR5 protein expression levels are influenced not only by variants in *CCR5* (*16*, *17*), but also by *CCL3L1* (Fig. 3C). Thus, virus × CCR5 × CCL3L1 interactions in vivo and the phenotypic effects associated with *CCR5* genotypes could depend, in part, on the genetic background conferred by *CCL3L1* dose. To test this hypothesis, we determined the phenotypic effects attributable to *CCL3L1* gene dose alone, *CCR5* haplotype pairs (genotypes) alone, and their combined effects.

The HIV$^+$ adult cohort was stratified into four mutually exclusive genetic risk groups (GRGs) based on possession of a population-specific low or high number of *CCL3L1* copies (*CCL3L1^{low}* or *CCL3L1^{high}*) and disease-accelerating, i.e., detrimental (det) or non-detrimental (non-det) *CCR5* genotypes (*CCR5^{det}* or *CCR5$^{non\text{-}det}$*) (Fig. 4A). Of the four GRGs, *CCL3L1^{high}CCR5$^{non\text{-}det}$* and *CCL3L1^{low}CCR5^{det}* were at the two extremes of HIV/AIDS susceptibility (Fig. 4, B to I). Relative to possession of *CCL3L1^{high}CCR5$^{non\text{-}det}$*, *CCL3L1^{low}CCR5^{det}* was associated with a ≥ threefold greater risk of progressing rapidly to 8 of 12 AIDS-defining illnesses (Table 1). By contrast, the *CCL3L1^{high}CCR5^{det}* and *CCL3L1^{low}CCR5$^{non\text{-}det}$* genotypes were associated with a ≤ threefold higher risk of progressing to 3 or 4 of these 12 illnesses, respectively (Table 1).

The trajectory of the frequency distribution profiles of the four *CCL3L1/CCR5* GRGs in individuals with varying follow-up times were also revealing in that they closely paralleled those described previously for a variable number of *CCL3L1* copies alone (compare Fig. 4J with Fig. 3, O and P, and fig. S7 to fig. S9). Thus, significant changes occurred only in the frequencies of the two GRGs that contained *CCL3L1^{low}* and *CCL3L1^{high}CCR5$^{non\text{-}det}$*, such that over time the distribution of the GRGs in surviving HIV$^+$ subjects approached ever closer to the values observed in the HIV$^-$ population (Fig. 4, J to L).

Taken together, in the context of a well-characterized prospective cohort composed of HIV$^+$ EAs and AAs, the *CCL3L1/CCR5*-based genomic signature for HIV/AIDS susceptibility was *CCL3L1^{low}CCR5^{det}* > *CCL3L1^{low}CCR5$^{non\text{-}det}$* ≥ *CCL3L1^{high}CCR5^{det}* > *CCL3L1^{high}CCR5$^{non\text{-}det}$*. This observation implied that *CCL3L1^{low}* may have a stronger effect than disease-accelerating, detrimental *CCR5* genotypes in influencing HIV/AIDS pathogenesis in these two populations. Additionally, these findings suggest that a population-specific low *CCL3L1* dose provides a permissive genetic background for the full expression of the phenotypic effects associated with detrimental *CCR5* genotypes. This was apparent because (i) relative to genotypes that contained only *CCR5^{det}*, those that contained *CCL3L1^{low}* with or without *CCR5^{det}* were associated with a higher risk of acquiring HIV (compare green with orange or red color-coded GRGs in Fig. 4, H and I); and (ii) the maximal disease-accelerating effects associated with detrimental *CCR5* genotypes occurred mainly in individuals who also possessed a low number of *CCL3L1* copies relative to the population-specific average (compare Kaplan-Meier plots for *CCL3L1^{high}CCR5^{det}* and *CCL3L1^{low}CCR5^{det}* in Fig. 4, E and F).

Public health impact of variations in *CCL3L1* and *CCR5*. In the populations examined, up to 42% of the burden of infection and ~30% of the accelerated rate of progression to AIDS were attributable to variations in

Table 1. Risk of AIDS-defining illness with *CCL3L1/CCR5* GRGs. The reference GRG for statistical analysis is C*CL3L1^{high}CCR5$^{non\text{-}det}$* (RH = 1). The AIDS-defining illnesses with sufficient events for statistical analyses recorded in the adult HIV$^+$ cohort are shown. CMV, cytomegalovirus; HAD, HIV-associated dementia; MAC, *Mycobacterium avium* complex; PCP, *Pneumocystis carinii* pneumonia; PML, progressive multifocal leukoencephalopathy; *n*, number of individuals with the indicated AIDS-defining illness; values in bold and italic indicate significant association.

AIDS-defining illness	*n*	*CCL3L1^{high}CCR5^{det}*			*CCL3L1^{low}CCR5$^{non\text{-}det}$*			*CCL3L1^{low}CCR5^{det}*		
		RH	95% CI	*P*	RH	95% CI	*P*	RH	95% CI	*P*
CMV infection	100	1.53	0.71–3.30	0.278	1.60	1.00–2.58	0.051	***6.21***	***3.63–10.63***	***2.7×10^{-11}***
Cryptococcosis	33	3.27	0.98–10.87	0.053	***2.46***	***1.00–6.02***	***0.048***	***8.11***	***2.93–22.46***	***5.6×10^{-5}***
Cryptosporidiosis	24	1.21	0.27–5.47	0.802	1.21	0.49–3.00	0.686	1.63	0.36–7.37	0.526
HAD	54	2.05	0.82–5.13	0.126	1.65	0.87–3.11	0.124	***3.18***	***1.33–7.60***	***0.009***
Herpes simplex	26	1.78	0.50–6.41	0.375	1.22	0.49–3.04	0.668	1.66	0.36–7.53	0.513
Histoplasmosis	20	3.32	0.83–13.30	0.090	***2.81***	***1.02–7.74***	***0.045***	1.56	0.19–13.01	0.682
Kaposi sarcoma	74	1.76	0.76–4.05	0.186	1.66	0.96–2.86	0.069	***3.86***	***1.90–7.83***	***2.0×10^{-4}***
Lymphoma	37	***2.87***	***1.10–7.48***	***0.031***	1.42	0.66–3.08	0.369	***3.38***	***1.21–9.43***	***0.020***
MAC	92	***2.22***	***1.09–4.55***	***0.029***	***1.73***	***1.05–2.87***	***0.032***	***5.13***	***2.79–9.45***	***1.5×10^{-7}***
PCP	196	***2.13***	***1.33–3.42***	***0.002***	***1.71***	***1.22–2.39***	***0.002***	***2.95***	***1.84–4.75***	***7.8×10^{-6}***
PML	18	1.72	0.36–8.10	0.494	1.27	0.44–3.67	0.657	2.41	0.51–11.43	0.268
Toxoplasmosis	27	1.49	0.32–6.91	0.610	1.69	0.67–4.25	0.268	***5.34***	***1.77–16.07***	***0.003***

CCL3L1/CCR5 (black bars in Fig. 5 and fig. S11). The largest contributor to the burden of HIV/AIDS was possession of a population-specific low *CCL3L1* copy number (Fig. 5, compare combination of red and orange to green bars, and fig. S11). These findings suggest that the contribution of *CCL3L1* copy number is comparable to or more than that of the *CCR5* genotype in influencing the epidemiology of HIV in the populations examined. These results also substantiate the observation that the disease-accelerating effects associated with variation in *CCR5* depend, in part, on the genetic background of *CCL3L1* copy number.

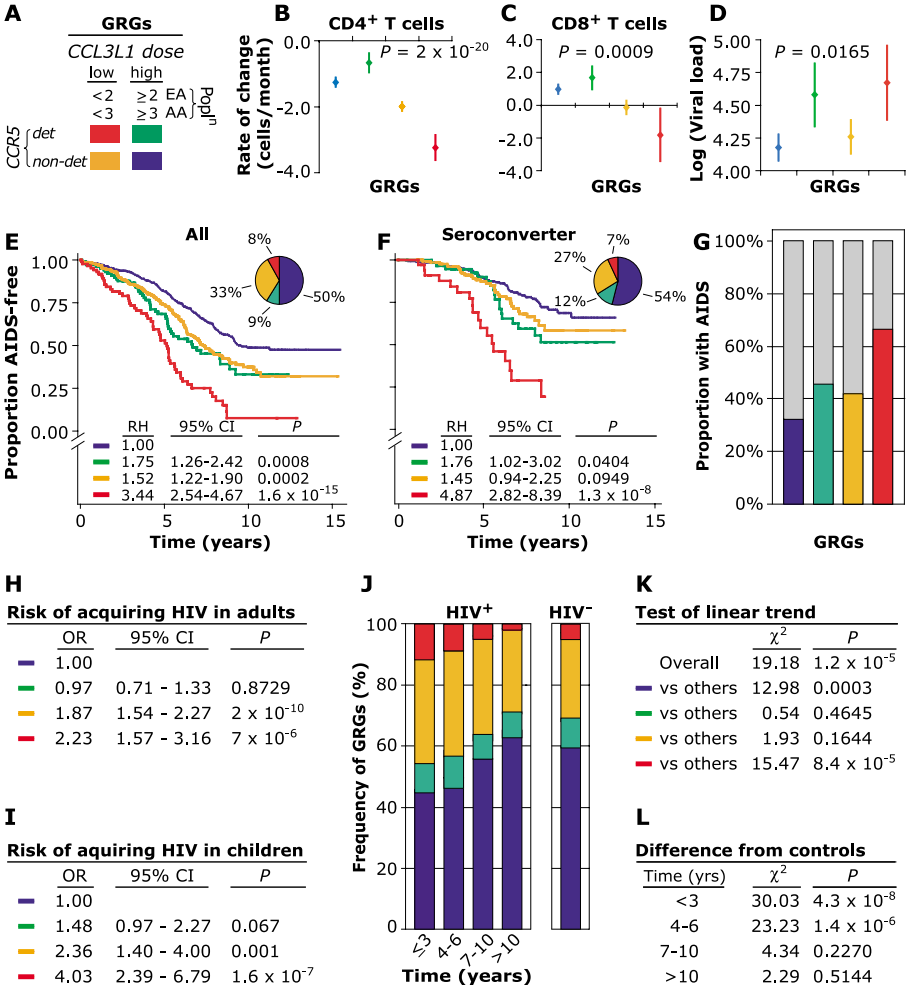

Fig. 4. Risk of acquiring HIV and disease-influencing effects associated with variations in *CCL3L1* and/or *CCR5*. (**A**) Genetic stratification system (SOM section 3). In each population (popl^n), *CCL3L1* dose and *CCR5* genotypes were dichotomized on the basis of whether they were associated with an accelerated disease course (tables S3 to S5). *CCL3L1^{low}* and *CCL3L1^{high}* denote copy numbers < or ≥ population-specific median, respectively (table S3). *CCR5^{det}* and *CCR5$^{non\text{-}det}$* denote population-specific, disease-accelerating, i.e., detrimental (*det*), or nondetrimental *CCR5* genotypes, respectively (table S4). Compared with possession of *CCL3L1^{high}* or *CCR5$^{non\text{-}det}$*, *CCL3L1^{low}* or *CCR5^{det}* was associated with an accelerated disease course (fig. S10). These dichotomized compound genotypes were used to stratify the cohort further into four mutually exclusive GRGs, which reflected (i) the independent disease-accelerating effects associated with population-specific low *CCL3L1* gene doses (*CCL3L1^{low}CCR5$^{non\text{-}det}$*, orange) or detrimental *CCR5* genotypes (*CCL3L1^{high}CCR5^{det}*, green); or (ii) their combined effects (*CCL3L1^{low}CCR5^{det}*, red), all relative to *CCL3L1^{high}CCR5$^{non\text{-}det}$* (blue). This color code is used in the rest of the panels to indicate the four *CCL3L1/CCR5* GRGs. (**B**) CD4$^+$ and (**C**) CD8$^+$ T cell changes associated with the GRGs are depicted as 95% CI around the point estimates of the regression coefficients obtained by the GEE method (*4*). (**D**) Baseline log viral RNA [viral set point; median (±1.7 SD of the median)] associated with the GRGs. *P* values reflect significance values for differences between *CCL3L1^{high}CCR5$^{non\text{-}det}$* and *CCL3L1^{low}CCR5^{det}* by Student's *t* test in (B) and (C) and the Mann-Whitney test in (D). (**E** and **F**) KM curves of the development of AIDS in EAs and AAs from the entire (E) or seroconverting portion (F) of the HIV$^+$ adult cohort after stratifying for the GRGs. (Inset) Pie charts depicting frequency distribution of the GRGs. (**G**) Proportions of individuals within each GRG that developed AIDS. (**H** and **I**) Association of indicated GRGs and risk of acquiring HIV infection in (H) adults or (I) children exposed perinatally to HIV. ORs are lowest in GRGs that lack *CCL3L1^{low}* (green). (**J** and **K**) Changes in the frequency distributions of the GRGs and test of linear trend for individuals with varying follow-up times. (**L**) Differences in the frequency distribution of GRGs between HIV$^+$ and HIV$^-$ adults. In (H) and (J), to ensure appropriate ethnic/racial matching for the comparisons of the frequency distributions between HIV$^+$ and HIV$^-$ individuals, these analyses are for the EA, AA, and HA portions of the infected adult cohort (tables S3 and S4; tables also show the genotypes used for the pediatric cohort in (I) (*4*).

Discussion. These findings have five major implications. First, they provide a precedent for a link between segmental duplication events leading to changes in the dose of an immune response gene and variability in the phenotypic response to an infectious disease. Recent human-nonhuman primate comparative genomic analyses have led to the prediction that genes embedded within segmental duplications might have enhanced the ability of humans to adapt to their environments (*1*, *18*). Our findings support this prediction.

Second, *CCL3L1* gene dose is a previously unrecognized means of buffering against the risk of HIV infection and/or disease progression in the populations examined. *CCL3L1* gene doses lower than the population-specific average provide a genetically "unbuffered" state with respect to the risk of HIV/AIDS susceptibility. However, it is important to emphasize that it is not the absolute gene copy number per se, but the copy number within the overall genetic context that confers phenotypic expression. This genetic context varies among populations as a result of their different demographic and evolutionary histories. Thus, an individual's specific *CCL3L1* gene dose and *CCR5* genotype are associated with susceptibility to HIV/AIDS, but only when viewed in the context of that person's geographical ancestry (Fig. 3Q) (*14*).

Third, within the populations examined, the Bradford-Hill criteria (*19*) for causality between *CCL3L1* dose and risk of acquiring HIV were met (SOM section 5.3). Thus, by analogy to the genetic studies that established the paradigm of "no CCR5–no HIV-1 infection," the current

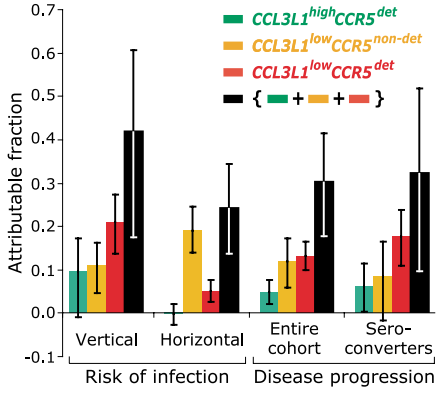

Fig. 5. Attributable fractions of *CCL3L1/CCR5* GRGs for risk of acquiring HIV (vertical, mother-to-child; horizontal, adult-to-adult) and rate of disease progression relative to *CCL3L1^{high}CCR5$^{non\text{-}det}$* in the indicated clinical settings. Vertical bars indicate the point estimate, whereas error bars represent the 95% CI around the point estimate of the attributable fraction.

findings establish that of "*CCL3L1*^{low}–enhanced HIV/AIDS susceptibility." These findings provide strong genetic underpinnings for the substantial body of evidence that CCR5 ligands play an important anti–HIV-1 role in vivo (*20*). Paradoxically, they also indicate that a network of HIV-suppressive CCR5 ligands (e.g., CCL5) cannot fully compensate for the functional state conferred by *CCL3L1*^{low}. Therefore, CCL3L1-mediated immune responses may be required to thwart HIV infection and the complications that occur during HIV-induced immune suppression.

Fourth, *CCL3L1* gene dose may be an important genetic correlate of vaccine responsiveness. A comparative analysis of the immunological phenotype linked to the GRGs associated with the extremes of susceptibility (i.e., *CCL3L1*^{low}*CCR5*^{det} and *CCL3L1*^{high}*CCR5*$^{non\text{-}det}$) could provide key insights into the immune correlates of an effective vaccine. This stems from several vaccine studies in simian models showing that CCR5 ligand production is a true predictor of protection and animals that produce higher levels of chemokines prevaccination exhibit greater protection (*20*–*22*).

Finally, and of broader import, 5% of the human genome contains duplicated sequences enriched for genes involved in immunity (*1*), and some of these genes have dosage effects. Thus, the present findings provide both a precedent and a framework for elucidating their relationship to human diseases.

References and Notes

1. J. A. Bailey *et al.*, *Science* **297**, 1003 (2002).
2. J. R. Townson, L. F. Barcellos, R. J. Nibbs, *Eur. J. Immunol.* **32**, 3016 (2002).
3. P. Menten, A. Wuyts, J. Van Damme, *Cytokine Growth Factor Rev.* **13**, 455 (2002).
4. Materials and methods are available as supporting material on *Science* Online.
5. J. W. Mellors *et al.*, *Ann. Intern. Med.* **126**, 946 (1997).
6. L. Wu *et al.*, *J. Exp. Med.* **185**, 1681 (1997).
7. D. Zagury *et al.*, *Proc. Natl. Acad. Sci. U.S.A.* **95**, 3857 (1998).
8. A. Garzino-Demo *et al.*, *Proc. Natl. Acad. Sci. U.S.A.* **96**, 11986 (1999).
9. J. Reynes, V. Baillat, P. Portales, J. Clot, P. Corbeau, *J. Acquir. Immune Defic. Syndr.* **34**, 114 (2003).
10. H. Ullum *et al.*, *J. Infect. Dis.* **177**, 331 (1998).
11. W. A. Paxton *et al.*, *J. Infect. Dis.* **183**, 1678 (2001).
12. J. Tang, R. A. Kaslow, *AIDS* **17** (suppl. 4), S51 (2003).
13. M. P. Martin *et al.*, *Science* **282**, 1907 (1998).
14. E. Gonzalez *et al.*, *Proc. Natl. Acad. Sci. U.S.A.* **96**, 12004 (1999).
15. A. Mangano *et al.*, *J. Infect. Dis.* **183**, 1574 (2001).
16. S. Mummidi *et al.*, *J. Biol. Chem.* **275**, 18946 (2000).
17. J. R. Salkowitz *et al.*, *Clin. Immunol.* **108**, 234 (2003).
18. R. V. Samonte, E. E. Eichler, *Nature Rev. Genet.* **3**, 65 (2002).
19. D. L. Weed, *Hematol. Oncol. Clin. North Am.* **14**, 797 (2000).
20. A. L. DeVico, R. C. Gallo, *Nature Rev. Microbiol.* **2**, 401 (2004).
21. J. L. Heeney *et al.*, *Proc. Natl. Acad. Sci. U.S.A.* **95**, 10803 (1998).
22. R. K. Ahmed *et al.*, *Clin. Exp. Immunol.* **129**, 11 (2002).

23. We thank the Board members and reviewers, including the statistical referee, for critically reviewing various aspects of this work and for very valuable suggestions; G. Crawford, B. Kasinath, G. Nabel, J. Burns, B. Cherniak, members of the Infectious Diseases division for helpful discussions and critical reading of the manuscript; E. Fattig and M. Hildebrand for technical assistance; N. Chopra and J. Sharron for graphic work; and A. S. Ahuja for forbearance. The Henry M. Jackson Foundation and the Military HIV Program, Walter Reed Army Institute of Research contributed support for the WHMC patient cohort as part of the Tri-Service HIV Program. Supported by the Veterans Administration Center on AIDS and HIV-1 infection, and grants from NIH (AI046326, AI043279, and MH069270) (S.K.A.). S.K.A. is a recipient of the Elizabeth Glaser Scientist Award and the Burroughs Wellcome Clinical Scientist Award in Translational Research. Because of space constraints, we regret our inability to cite additional excellent work. The views expressed herein are those of the authors and do not reflect the official policy of the Department of Defense or other departments of the U.S. government.

Supporting Online Material

www.sciencemag.org/cgi/content/full/1101160/DC1
Materials and Methods
SOM Text
Figs. S1 to S16
Tables S1 to S7
References and Notes

7 June 2004; accepted 22 December 2004
Published online 6 January 2005;
10.1126/science.1101160
Include this information when citing this paper.

REPORTS

The Geometric Distance and Proper Motion of the Triangulum Galaxy (M33)

Andreas Brunthaler,[1,2]* Mark J. Reid,[3] Heino Falcke,[4,5] Lincoln J. Greenhill,[3] Christian Henkel[1]

We measured the angular rotation and proper motion of the Triangulum Galaxy (M33) with the Very Long Baseline Array by observing two H_2O masers on opposite sides of the galaxy. By comparing the angular rotation rate with the inclination and rotation speed, we obtained a distance of 730 ± 168 kiloparsecs. This distance is consistent with the most recent Cepheid distance measurement. M33 is moving with a velocity of 190 ± 59 kilometers per second relative to the Milky Way. These measurements promise a method to determine dynamical models for the Local Group and the mass and dark-matter halos of M31, M33, and the Milky Way.

Measuring the proper motion and geometric distances of nearby galaxies has been a long-standing problem. As part of a famous debate about the nature of galaxies, van Maanen—an experienced observer—claimed in 1923 to have measured a large proper motion and angular rotation rate for the Triangulum Galaxy (M33) on photographic plates separated by 12 years (*1*). These results were proven incorrect by Hubble through the discovery of Cepheids in M33 that showed a large distance (*2*). Measuring proper motions at this large distance was beyond the capabilities of their time. This pushed the detection of galaxy proper motions beyond the capabilities of past experiments. Yet galaxy proper motions are important for many astrophysical issues, of which two are addressed in this report.

First, measuring accurate distances is of great importance to all fields of astrophysics, from stellar astronomy to cosmology. The calibration of most standard candles used for measuring extragalactic distances is tied directly or indirectly to the distance to one galaxy, the Large Magellanic Cloud (LMC), which remains controversial (*3*, *4*). Hence, it is important to obtain geometric distances to nearby galaxies in which well-understood standard candles can be studied. This allows independent calibration and verification of the extragalactic distance scale.

Another important issue is the distribution of luminous and dark matter in the local universe. The problem when trying to derive the gravitational potential of the Local Group of galaxies (*5*) is that usually only radial velocities are known from the Doppler effect and statistical approaches have to be used (*6*, *7*). The proper motions of some nearby galaxies in the Milky Way subgroup have been obtained from comparing historic photographic plates (*8*, *9*), but a confirmation

[1]Max-Planck-Institut für Radioastronomie, Auf dem Hügel 69, 53121 Bonn, Germany. [2]Joint Institute for Very Long Baseline Interferometry in Europe, Postbus 2, 7990 AA Dwingeloo, Netherlands. [3]Harvard-Smithsonian Center for Astrophysics, 60 Garden Street, Cambridge, MA 02138, USA. [4]ASTRON, Postbus 2, 7990 AA Dwingeloo, Netherlands. [5]Department of Astrophysics, Radboud Universiteit Nijmegen, Postbus 9010, 6500 GL Nijmegen, Netherlands.

*To whom correspondence should be addressed. E-mail: brunthaler@jive.nl